CONTROL SYSTEMS LABORATORY

ASSESSMENT OF ANTENNA IMAGE QUALITY
BY A MECHANICAL OBSERVER

Report R-110

December 1958

Contract DA-36-039-SC-56695
D/A Sub-Task 3-99-06-111

UNIVERSITY OF ILLINOIS · URBANA · ILLINOIS

The research reported in this document was made possible by support extended to the University of Illinois, Control Systems Laboratory, jointly by the Department of the Army (Signal Corps and Ordnance Corps), Department of the Navy (Office of Naval Research), and the Department of the Air Force (Office of Scientific Research, Air Research and Development Command) under Signal Corps Contract DA-36-039-SC-56695.

ASSESSMENT OF ANTENNA IMAGE QUALITY BY A MECHANICAL OBSERVER

by

J. J. Myers

Report R-110

December 1958

CONTROL SYSTEMS LABORATORY
UNIVERSITY OF ILLINOIS
URBANA, ILLINOIS
Contract DA-36-039-SC-56695
D/A Sub-Task 3-99-06-111

SUMMARY

An experimental evaluation of the effect of aperture illumination on the resulting image of a high-resolution antenna was made using a mechanical observer for assessing quality. The mechanical observer consisted of ILLIAC, the University of Illinois digital computer, programmed for the purpose. The evaluation was intended to complement an experimental evaluation of antenna image quality made by human observers, as described in CSL report R-109, and a mathematical study of quality criteria reported in CSL report R-108.

A close connection between image quality and aperture illumination was found by the mechanical observer as measured by its ability to analyze the images presented to it for assessment. The data show that a uniform aperture illumination is close to optimum. This result agrees with the result obtained in the experiment of report R-109.

Results obtained from an assessment of a representative class of aperture illuminations are presented, and a detailed description of the mechanical observer and a block diagram of the logic used are given.

ACKNOWLEDGMENT

The use of the ILLIAC as a mechanical observer for assessing antenna image quality was suggested by Dr. J. P. Ruina of this laboratory. Acknowledgment is made of the help given by Mr. Donald Bitzer during the early stages of development of the mechanical observer.

The report contains extracts from a dissertation submitted in partial fulfillment of the requirements for the Ph.D. degree at the University of Illinois.

TABLE OF CONTENTS

LIST OF FIGURES

I. INTRODUCTION

General

This report is the third of a group of three reports giving the results of a theoretical and experimental study of antenna resolution and image quality as related to aperture illumination. The first part of the study[1] was an investigation of mathematical quality criteria used for evaluating antenna images; the second part[2] was an experimental evaluation of antenna image quality making use of an optical simulation technique and human observers; and the third part, reported here, was an experimental evaluation of antenna image quality making use of a mechanical observer.

Briefly, the objective of the study was to evaluate the effect of changes in aperture illumination on the resolution and image-quality performance of large-aperture antennas. Considerable background material is given in the two reports referenced above and is not repeated here.

Mechanical Observer

For purposes of the study, a mechanical observer was a device used in lieu of a human observer for assessing antenna image quality in an "objective" way. Such an observer appears never to have been used before for this purpose.

In contrast to a human observer, a mechanical observer, particularly when it uses digital techniques as in this study, is for all practical purposes a perfectly constant observer and so can be made to

1. Myers, J. J., "Antenna Image Quality Criteria", Control Systems Laboratory Report R-108, Univ. of Illinois, Urbana, Ill.; Dec. 1958.
2. Myers, J. J., and B. D. Elliott, "Optical Simulation of Antenna Images", Control Systems Laboratory Report R-109, Univ. of Illinois, Urbana, Ill.; Dec. 1958.

apply any chosen criterion of image quality in a constant manner. In particular, the application of the criteria can be completely invariant with changes in antenna aperture illumination and with time. As compared with a human observer, an MO (mechanical observer) is more constant, is not subject to fatigue, is much faster, requires no training, and is independent of the physiological and psychological factors that influence a human observer. Further, since the criteria applied by the MO are subject to precise numerical control, very small differences in images and hence image quality that arise from small changes in aperture illumination are observable.

Any MO must operate within a framework defined by the specific rules arbitrarily chosen by the designer. Since it cannot exercise judgment beyond that anticipated and provided for by the designer, an MO reflects his ideas of what is an appropriate logical design. This fact does not necessarily detract from the value of the results so long as the MO's rules of observation are indeed invariant with time and with aperture illumination. No attempt was made in the development of the MO to design an optimum observer; this problem was outside the scope of the present study. Instead, the design procedure was adopted which would lead to a useful observer, within the context of the definition of the problem to be studied, and attention was concentrated on making the observer flexible and reasonably efficient.

The use of an MO for image evaluation has an important significance in light of the tendency today to mechanize as many system functions as possible, including the observer or decision-maker. This tendency arises from the fact that the output data rates are rapidly rising and increasingly makes it difficult or impossible to incorporate humans, with their limited capacity in terms of information bits per second, in complex systems. If an antenna image is ultimately to be analyzed by

mechanical means, then the system parameters, including aperture illumination, should be chosen to maximize the probability of extracting from the image the desired information. Accordingly, although the mechanical observer developed for this study may not represent an optimum type for a practical system, mechanical evaluation has a sound basis in today's technology, and the results obtained from the experiment give a great deal of insight into how the performance of an MO is affected by the antenna pattern of the system.

Task of Mechanical Observer

The problem presented to the MO was that of analyzing, or "deconvolving"[3] into its constituent parts, a given waveform, e.g., Fig. 1, constituting the image being assessed. In this case, the image was nearly perfect in the sense that it was obtained analytically and computed numerically to a high degree of precision. For the analyses there were chosen images of the same representative class used for the preceding theoretical and experimental studies, viz., the class of illuminations described in Appendix B of CSL Report R-108 given by $(1 + A \cos 2x/L)$, where x is the aperture coordinate, L is the antenna length, and A is an aperture illumination parameter defined over the interval (-1, 1). Throughout the analyses, nothing except the aperture illumination factor, A, was changed in measuring the effectiveness of deconvolution as a function of the aperture illumination.

It may be shown that there is no unique solution possible in the deconvolution process, for there is an infinite set of possible

3. The manufactured term "deconvolution" is used because it is descriptive of the inverse operation by which the image was obtained, i.e., the inverse of convolution of the antenna pattern and the object distribution. The quotation marks around the word will be dropped in subsequent use in this chapter and in the Appendix.

target[4] configurations that could give rise to the type of image envelopes presented for analysis. However, since it was not required of the MO that it perform a perfect deconvolution of the image, a satisfactory solution for purposes of this study was obtained for an appropriate variety of target dispositions.

In assessing the quality of the images presented to it for analysis, the MO was "unaware" of the contents of the image beyond "knowing" that it was formed by convolution of a given antenna pattern and some unknown disposition of point targets. Stated differently, this is to say that the MO was presented with the image envelope only (in the form of a set of values of ordinates, Fig. 4, equispaced across the image, i.e., the received amplitude of the signal for discrete values of time) and hence it had no more information about the probable contents of the image than might be given a human observer performing the analysis in the same way. How well the deconvolution was performed was taken as a measure of the quality of the image. For purposes of assessment by the MO the best image was that image which was most easily deconvolved.

The MO developed[5] has potential use in the practical analysis of real data, such as that obtained from a radio telescope. Although the MO was applied to analyzing artificial images, no restriction to artificial data is thereby implied.

---

4. Borrowing a term from radar, the word "target" will be used to denote a radiating or reradiating object which gives rise to a corresponding image, even though the "target" is in fact a self-luminous object, such as a radio star.
5. The MO consisted of ILLIAC, the University of Illinois digital computer, and a suitable program that gave rules of observation, such as might be given a human observer performing the analysis in the same (although much slower) way.

II. PROCEDURE

Manufactured Images

The image produced by a scanning antenna is in the form of an output voltage that varies with time as the antenna scans a set of radiating or reradiating objects. When point objects that radiate incoherently with respect to each other are scanned, the antenna output power is the sum of the powers due to each object individually. One may manufacture equivalent images by linearly summing the responses of a given imaging system to some assumed distribution of point targets. The resulting simulated antenna image is very much like images obtained from an antenna scanning real targets of the same type.

For the purpose of forming images for mechanical analysis by the MO, the above-described method of image manufacture was employed. The actual computations were made by ILLIAC according to a program prepared for the purpose. The results of the computation were stored within the memory of ILLIAC. In Fig. 4 is shown a representation of the type of data manufactured, and in Fig. 2 are shown photographs of the ILLIAC cathode-ray tube output for typical images.

In order to form the images, it was necessary to specify for each image the aperture illumination factor, A, the spacing between ordinates, the total number of ordinates to be computed, the location and relative amplitudes of the targets (as many as 100 could be handled in a single image), and the signal-to-noise ratio desired, if optional noise in the form of random numbers was to be added to the completed image (see Fig. 3b).

The calculation of the image by ILLIAC was done on an ordinate-by-ordinate basis, the total ordinate due to contributions from each of the targets specified being computed during one cycle through the

appropriate loop of the program. In addition, following computation of the image (Fig. 4b), a reference antenna power radiation pattern (Fig. 4a) was computed in the same manner and stored at a separate location. This reference pattern was used by the MO in the manner described below.

If the MO was to have been used on real data instead of on manufactured images, the values of the received signal at equal time intervals would have been inputed directly into the appropriate location of the ILLIAC memory. Also, the measured values of the antenna radiation pattern at the same interval used for the image would have been inputed into the appropriate place of the memory.

Observer Design

The MO design was based on a curve-fitting technique by means of which the images of the individual targets were successively removed from the original image until the residual was reduced to some arbitrarily chosen threshold. The curve-fitting was applied first in successive stages of approximation to the largest target of the image; when the best estimate of its position and amplitude was determined, the image of this target was removed from the original image and the process was continued until all targets had been located. When the blending or smearing of one target's image into another was not great, deconvolution of the image was done easily and accurately by the MO; when the blending was severe, deconvolution was poorer until for an excessive amount of blending the MO was unable to analyze the image into its component targets satisfactorily.

The deconvolution process employed for the MO is complex and is described in detail in the Appendix. The following six paragraphs give the essentials of the process:

(1) The approximate positions of suspected targets were determined by a simple peak-picking technique. The largest of such suspected targets (Fig. 4b) was then assumed to be the largest target present.

(2) In order to minimize the smearing effect on this largest target due to nearby targets, the nearby targets were removed to leave a more-or-less well defined peak (Fig. 4c) that was assumed to be a more nearly true representation of the largest target.

(3) To this largest target was fitted on a least-squares basis the main lobe of the reference antenna pattern (Fig. 4a) over the half-power width. The best fit was taken as defining tentatively the true location of that target. The estimated target size and location were saved for later use.

(4) This largest target was then removed from the original image (meanwhile preserving elsewhere in the computer memory the original image).

(5) The entire process of steps (1) through (4) was repeated successively on the remaining image to find the next largest target; and so on until finally there remained no potential targets greater than the threshold that had been chosen.

(6) Following the removal of all targets above the threshold, the steps (1) through (5) were repeated using the target estimates obtained previously. Upon applying the curve-fitting procedure a second time, the resulting estimates of position and amplitude of the targets were improved because of there having been subtracted from the vicinity of the targets being fitted more nearly the correct interfering targets.

Fig. 2 shows the deconvolution of a three-target image in graphic form indicating the condition of the image at each subtraction step. In (a) of the figure is a typical noise-free image. In (b) through (d) are the results of going through the first major cycle of the deconvolution process, removing the targets during the cycle in decreasing order of their amplitudes. It may be noted in (d) that the residual remaining is not insignificant and that it exists because of inaccurate estimates of the true sizes and positions of the targets.

The result of going through the second major cycle of the deconvolution process is shown in (e) through (g) of Fig. 2. It may be seen that the final residual left after subtracting each of the three targets present is appreciably less than the residual left in the earlier steps

of the first major cycle. In some cases, e.g., the image shown in Fig. 2, further repetitions of the steps of the second major cycle could have reduced the residual arbitrarily low. However, for the purposes intended, there was little reason to look for extremely small residuals. In practice, the threshold was set to allow a residual of 10%.

The method chosen for curve-fitting was the univariate,[6] or one-at-a-time, method of arriving at a minimum corresponding to the best fit. The sum of the squares of the differences between the ordinates of the target and ordinates of the main lobe of the reference antenna pattern was used as a measure of the fit. When this sum had been reduced as low as possible by varying the parameters in the fit, the fitting process was terminated. In fitting the main lobe to the assumed target, there was added a d-c term, or pedestal, to take into account contributions to the image due to blending from other targets or due to noise. During a fitting cycle, each of the three parameters, viz., the main lobe amplitude, its position, and the value of the d-c term, were varied one-at-a-time until the sum of the squares of the differences was minimized.

Observer Errors

Errors in the deconvolution process arose only from inexact estimates of the target locations and sizes since ILLIAC does essentially perfect subtraction, i.e., exact to at least 11 decimal places. An indication of the magnitude of the errors introduced is given in Fig. 5. In (a) is plotted for a typical aperture illumination (uniform) the absolute value of the shift in the apparent position of a target, i.e., the shift in the location of the maximum ordinate, due to the proximity

6. Box, G. E. P., and K. B. Wilson, "On the Experimental Attainment of Optimum Conditions", J. Roy. Stat. Soc., v. 13B, pp. 1-45; 1951.

of another target, for several different target amplitude ratios. Beyond a target spacing of about 1.0 there is plotted only the error curve for 1:1 target ratio; for the other ratios, the curves would each fall below that for 1:1.

Referring still to Fig. 5a, it is apparent that when two targets are sufficiently close they merge and the maximum ordinate of their sum occurs somewhere between the two targets. At this spacing, the position of the maximum ordinate is halfway between the two targets when the target amplitude ratio is 1:1. As the targets are moved apart, the distance between the maximum ordinate and the location of either of the two targets increases, always remaining equal to half of the spacing between the targets. At a certain spacing, the composite image will show two peaks corresponding to the two targets, and the position error becomes much smaller than for the closer spacings. Inasmuch as the simple peak-picking procedure used to obtain the first estimates of the correct positions of the suspected targets is based upon the position of the maximum ordinate, it is apparent that the potential error in this estimate may be considerable, at least when the main lobes of the two images interfere. As the targets are moved further apart, it is only the sidelobes which interfere to cause a shift in apparent position of the targets, although for high sidelobes the perturbation of the main target due to the sidelobes may be large for certain target spacings.

In Fig. 5b there is given a plot of the maximum residual ordinate left in the subtraction process when the target response subtracted is in error in amplitude and in position. When the error in position, for example, is zero, then a 5% error in amplitude results in a 5% subtraction residual. When for the same amplitude error the error in position is as much as 10% of a half-power beamwidth, then the residual rises to

only 12.5%. Examination of Fig. 5 reveals that the subtraction process is relatively insensitive to errors in estimated position, but that it is highly sensitive to errors in estimated amplitude. Typically, the errors in the estimate of the position in the analysis of images made during this study were of the order of only 1/50 of a half-power beam-width; the amplitude errors ranged up to as much as 50% when the blending in the images was great.

From the above discussion, it may be concluded that for accurate deconvolution in the process used for the MO, it is more important that the amplitude estimates be good than that the position estimates be good.

Observer Operation

Prior to using the MO it was necessary to manufacture an image, as described before, and a radiation pattern (point object response) of the antenna being simulated. The set of calculations of the ordinates of the image were stored at two different locations in ILLIAC. The first set of ordinates was used for obtaining the tentative estimates of target positions and amplitudes during the first major cycle of operation of the MO; the second set was used for the second major cycle to obtain the final estimates.

Following manufacture of the image, the MO program was read into the computer and, with the running switch set to bypass optional stops in the program, ILLIAC would without operator attention go through a complete deconvolution cycle for the image presented for analysis, meanwhile displaying at appropriate stages the condition of the image. By means of the display (on a Hughes Memotron long-persistence cathode-ray tube) it was possible to watch the course of the deconvolution and to see which target was found and subtracted at each point in the process.

Prior to starting the actual image analysis, the MO measured (1) the antenna pattern half-power beamwidth, which established the region over which the curve-fitting was done; (2) the 90% width of the main lobe, which established a constant for the criterion used to determine which peak in the image constituted a potential target; and (3) the highest sidelobe level of the pattern to set a threshold for selection of neighboring peaks. After setting the constants on the basis of these measurements, the main MO program took over. At each state where an estimate of the presence of a target was made, the results were recorded on punch tape which could be printed at the conclusion of the analysis.

In Fig. 13 is shown the printed output from the MO for a two-target image. The identification of the image is given by the serial number (e.g., SER 249); the value of the antenna illumination factor, A, is indicated next, (e.g., -0.5); then follows identification of the noise, if any, added in terms of the value of r-m-s noise to peak signal ratio, plus a digit to indicate the particular series of random numbers used. This data described above and the column headings constituted the heading for an analysis.

Following the heading are four estimates of correct amplitude and position for each of the two targets, the value of the d-c pedestal added (CONST), and the number of trials (TT = times through) required to arrive at the best fit. The final, or fourth, estimate is the best estimate.

Experimental Design and Scoring

Experimentally it was determined that the accuracy with which deconvolution of images was carried out was directly proportional to the number of trials made during the curve-fitting procedure. That

this proportionality should exist is seen when it is recognized that the number of trials is dependent upon the flatness of the minimum being sought and upon the correctness of the initial estimate of the value of parameters associated with the minimum. In turn, the correctness of the original estimates of the best values for the parameters used to start the curve-fitting were inversely proportional to the degree of blending of the images of the individual targets, i.e., a large amount of blending led to poor first estimates. Also, the more the blending the flatter the minimum on the three-dimensional "surface" over which the best-fit search was carried out.

The total number of trials required to reduce the residual in the image to the 10% level was taken as the measure of the quality of the image. In order to arrive at an average quality, there was used as the measure the number of trials for deconvolving two-target images, averaged over target spacings varying from those which gave essentially perfect deconvolution to those which were impossible for the MO to deconvolve. The validity of this procedure was verified experimentally by deconvolving images containing a large number of randomly disposed targets of random amplitude and noting that the number-of-trials measure correlated well with the accuracy with which the targets were located. However, in the final evaluation there were used two targets only because the number of parameters involved were sufficiently few to permit a complete analysis to be run in acceptable time.

If the MO knew that the image was made up of the responses from two targets alone, then it would be a relatively simple matter to deconvolve the results with a high precision, regardless of the target spacing, by means of a modification of the curve-fitting employed, viz., by fitting the syspected peak to a curve made up of the sum of two impulse responses, the best fit being obtained by adjusting a total of four

parameters by the univariate (or other) method. Inasmuch as this knowledge was not imparted to the MO, it made its own determination of the number of targets present. In some cases, it decided that it was not capable of deconvolving with acceptable precision and hence it found no targets; in other cases it found either fewer or more targets than actually were present. Finding other than the correct number of targets implied a partially unsatisfactory deconvolution and this fact was reflected in the number of trials required to reduce the residual to the arbitrary threshold.

In using the number of trials as a criterion of image quality, it would not be expected that the graph of the number of trials vs. target spacing would be continuous. A discontinuity occurred, in fact, for the target spacing at which the number of targets found changed; the location of the discontinuity depended upon the setting of the threshold. However, in the evaluation carried out and reported below, the range of target spacings used did not include discontinuities.

The MO was applied to the analysis of two-target images formed with antenna aperture illumination of the same class used in the analytical work of CSL Report R-108 and in the optical study of CSL Report R-109. Values of the parameter, A, were chosen as -1.0, -0.5, 0, 0.5, and 1.0. Target spacings varying from Rayleigh[7] for A = 1.0 to about 2/3 Rayleigh for A = -1.0 were used in finding the average performance. Target amplitude ratios of 1:1, 1:2, and 1:5 were chosen. This range of spacings was chosen since spacings greater than these gave essentially perfect deconvolution regardless of the aperture illumination, whereas smaller spacings were not analyzable by the MO for all illuminations. In the analyses, noise-free images were used.

7. See the Rayleigh Spacing Criterion of CSL Report R-108.

III. RESULTS

A total of 108 analyses of images were made in arriving at the data and conclusions discussed below. The results are presented in the plots of Figs. 6-12.

Figs. 6-10 show, as a function of target spacing for each of the five aperture illuminations, the positional error and amplitude error found for each of the two targets. These data are given to support the use of the number-of-trials, also shown in the same figures, as a measure of overall image quality. The correlation between the number-of-trials plot and the resulting errors in position and amplitude (especially the latter) is apparent. All data do not extend over the entire range of target spacings because of catastrophic failures, that is, failure of the MO to find targets. For example, in the 1:1 amplitude plots the individual curves terminate at about that point where further decreasing of the distance between the targets results in no data, i.e., the MO finds no targets. This failure to find targets occurs when the shape of the composite image due to the two targets becomes too broad in the main-lobe region for the MO to determine that there is a legitimate target present.

Fig. 11 summarizes the results for 2:1 and 5:1 target ratios. The results for 1:1 amplitude ratios are not displayed because the range of deconvolvability was sufficiently different for the various aperture illuminations that insufficient data was obtained to form a plot of the type given for the other amplitude ratios. In the figures, the relative effort required by the MO to reduce the residual to the 10% threshold is given for various target spacings. It is apparent (in Fig. 11) that for target spacings approaching the minimum the effort required to deconvolve the image was proportional to the expected resolvability

based on main-lobe beamwidth. It is also apparent that the effort required was related to the interference between sidelobes and main lobe, e.g., witness in Fig. 6c the relatively large effort required in the A = -1.0 case for target spacings near 0.75.

The overall summary curves of the image assessment performed are in Fig. 12. In (a) is plotted the overall quality obtained by taking the average of the data of (c) in Figs. 6-10 over the target spacing from 1.0 to 0.25. This plot gives the average difficulty of deconvolving the images analyzed. As plotted, the data have been normalized so that unity represents the best performance relative to the data displayed. It is quite clear that the optimum performance occurs for that aperture illumination which is nearly uniform, i.e., near to A = 0. In Fig. 12b are resolution curves which indicate the approximate location of the minima of the curves of Fig. 11 as a function of aperture illumination factor. These curves have been normalized so that unity represents the best illumination of the class. As would be expected, the best resolution occurs for values of A near to -1.0; the broken portion of the curve indicates that for normalized quality factor less than 0.4 (which represents target spacings <u>greater</u> than 1.0), the resolvability by the MO measure is independent of aperture illumination. This is to say that for such target spacings the MO was able to resolve the targets essentially perfectly regardless of the aperture illumination.

IV. CONCLUSIONS

It is evident from the data that there is a significant difference between the various illuminations used insofar as the resulting deconvolvability of the image is concerned. Hence, there is to be expected a significant variation in performance of a mechanical observer as a function of the aperture illumination used.

The data of Fig. 12a show that a uniform aperture illumination is close to optimum. This result agrees with the result obtained in the optical experiment of CSL Report R-109, although the two experiments were quite different and would not necessarily be expected to yield the same result. The result of Fig. 12b, showing that best resolvability indeed occurs for the narrowest beamwidth, in part validates the results obtained for overall image quality by showing that the analysis of image quality was not in error from the resolution aspect.

APPENDIX

Mechanical Observer Design

General

The design of the mechanical observer employed may be understood by referring to the following description of the logic used and to the block diagram of Fig. 14.

The program for the mechanical observer is in three main parts: (1) a preliminary program, which is erased after being used at the beginning of the image analysis; (2) a loop used in the first major cycle for obtaining the first, second, and third estimates of target positions and sizes; and (3) a loop used in the second major cycle for obtaining the fourth and final estimates of the targets present in the image.

Logical Design

General

The design of the mechanical observer used is based upon a deconvolution[3] scheme which involves finding in the image to be analyzed point targets according to certain criteria of what constitutes targets. Upon finding a target and making repeated estimates of its correct position and amplitude, the target is removed from the image and the entire process repeated until all targets above a given threshold have been removed.

The choice of numerical values for various parameters is arbitrary; the values were, in fact, selected empirically following considerable exercising of the mechanical observer and experimental studies of proper choices of values.

Preliminaries

The computed antenna pattern, Fig. 4a, (or pattern loaded from numerical values, in the case of real data) is examined and the width, w, of the main lobe at 90% amplitude, the width, W, at the half-power points, and the height, y_o, of the first sidelobe are determined. The use of these measurements is given below.

First Major Cycle

(1) The image (Fig. 3b in the case of noisy data, or Fig. 3a in the case of noise-free data) is smooth by a running sum technique, i.e., by summing N ordinates and normalizing by N to get an ordinate for the smoothed image whose abscissa is taken to be that of the center of the group of N (an odd number). Expressed analytically, there is formed the sum

$$\frac{1}{N} \sum_{j=i}^{i+N} y_j \qquad 0 \leqslant i \leqslant (M - N)$$

which, upon being taken successively over the entire image, gives a new image (Fig. 3c) defined over the range $N \leqslant i \leqslant (M - N)$. M is the total number of ordinates in the original image, and y_j is the amplitude of the jth ordinate. It may be noted that this type of smoothing is equivalent to performing a convolution between the image and a rectangular pulse of width equal to the smoothing interval, N. This smoothing, of course, distorts the image somewhat, the amount depending upon the smoothing interval used. However, inasmuch as later curve-fitting is done to the original image rather than to the smoothed image, the smoothing has no effect upon the quality of fit obtainable. An alternative procedure would have been to smooth the image and fit it to a smoothed antenna pattern; for several reasons this method was not chosen.

In practice, the smoothing is not required for noise-free images, although to avoid the complications of having different procedures for noisy and noise-free images, smoothing is applied to all images. In performing the smoothing, the original data is preserved intact for later reference.

(2) The maximum ordinate, y_{max}, of the smoothed image is found and used to establish a threshold, t, below which target hunting is not to be done (Fig. 4b). The maximum ordinate is also taken to be the first estimate of the location and size of the largest target in the image.

(3) The peaks in the smoothed image within a distance of $\pm$ a of the largest ordinate (Fig. 4b) are found. A simple criterion determines what constitutes a legitimate peak: the values of the ordinates at a distance equal to one-half the 90% width, w, on each side of the ordinate being investigated are required to be no greater than 0.9b times the maximum ordinate ($1 \leqslant b \leqslant 1.1$). If more than one ordinate satisfies this criterion within an interval that is the width of the smoothing interval, N, used in (1) above, then only the largest of the ordinates is taken as representing the approximate location of a peak. No peak below the threshold, t, set in (2) and no peak below some multiple, α, of the sidelobe level, y_o, is considered a valid peak.

(4) Without destroying the original image, there is subtracted from the vicinity of the maximum ordinate corresponding to the largest target the image contributions due to the nearby targets found in (3). This is illustrated in Fig. 4c which shows how the largest target is revealed relatively unencumbered after subtraction. The nearby target image contributions are subtracted over a region sufficiently broad to allow curve-fitting over the half power width, W, of the main lobe.

(5) The unencumbered image obtained in (4) is then fitted to the main lobe of the antenna reference pattern in order to find a better

estimate of location and amplitude of the target that is given from the estimate obtained in (2). The fitting is done by finding and minimizing the mean square error between the section of image (Fig. 4c) and main lobe of the reference pattern (Fig. 4a). Expressed analytically, there is formed and minimized the sum

$$\sum_{j=W/2}^{W/2} \left[y_j \text{ image} - (y_1 + \beta y_{(j+n) \text{ ref. fn.}}) \right]^2$$

where the index, j, is taken with reference to the estimate made in (2); n is a parameter which is varied to adjust the position of group of ordinates in the reference pattern used during the fitting; y_j is the ordinate; W is the half-power width of the reference pattern, as found in the preliminary program; y_1 is a d-c term, or pedestal, added to account for contributions to the image due to noise or unsubtracted targets; and β is the amplitude parameter. During fitting, the three parameters n, β, and y_1 are adjusted by the univariate, or one-at-a-time, method[6] to minimize the sum. The bin size used, relative to y_{max}, is initially 2% for k, 0.5% for y_1, and 15 for n; after finding the best fit for a given bin size, the bin is reduced in size 50%, and so on until the final bin size is 1/16 of the starting size. The values of n, β, and y_1 at the time curve-fitting is terminated are used to form a new y_{max}, x_{max}, and y_1 for the amplitude, position, and d-c term, respectively, of the second estimate.

(6) The third estimate is formed by modifying the second estimate so that the new-estimate amplitude is the sum of the d-c term and the previous estimated amplitude. This modification proved desirable since peak-broadening due to perturbations of nearby targets resulted in amplitude estimates that were more nearly the sum of the two terms used

than they were the second estimate amplitudes. Thus, the third estimates, stored in the memory for later use, are not truly new estimates.

(7) Based on the third estimate, there is removed from the original image the image of a target of the size and at the position indicated. This removal results in a new image that differs from the original only in the absence of the largest target. The original image is still retained unchanged for later use. This removal is shown in Fig. 2b. It is apparent that "hidden" targets are uncovered by this technique.

(8) The remaining image is then re-entered and treated as the original image through steps (1) and (7), except that the threshold, t, of step (2) is not reset. The process is continued until there remains no ordinate above the threshold, t, or until there are no legitimate peaks found in (3). This procedure constitutes the first major cycle of the program.

Second Major Cycle

(1) Upon failure of the threshold test of (8), the second major cycle is entered and various modifications in the program instructions are made as required.

(2) The list of third estimates stored in (6) above is examined and the largest estimated target selected. The estimates of other targets within the vicinity $\pm$ a of this largest target are used to determine targets to be subtracted from the original image, which had been preserved intact throughout all of the above steps in the same manner as done in (4) of the first major cycle.

(3) Following the same procedure of (5) above, curve-fitting by the minimum square error criterion is done to obtain an improved estimate of the location and amplitude of the largest target; these estimates constitute the fourth and final estimate.

(4) As done in (6) above, the largest target is removed from the original image (Fig. 2e) to leave a modified image that is treated again as the original image.

(5) The next largest target in the stored list is selected, as in (2), and steps (3) and (4) are repeated; and so on until all targets in the list have been used. The result is a residual (Fig. 2g) which, in general, is less than the residual left after the first major cycle (Fig. 2d). This second-time-through process improves the accuracy of the estimates in most cases, further iterations of the process could, in most cases, improve the estimates further, although it was not felt justified for the present purposes.

The analysis of the 108 images used in obtaining the results presented required a total of about 30 hours of actual computer operating time, including the manufacture of images (a total of perhaps 100 computer operating hours were required during the development of the program and initial exercising of the MO). Many hundreds of images were analyzed by the MO during its development.

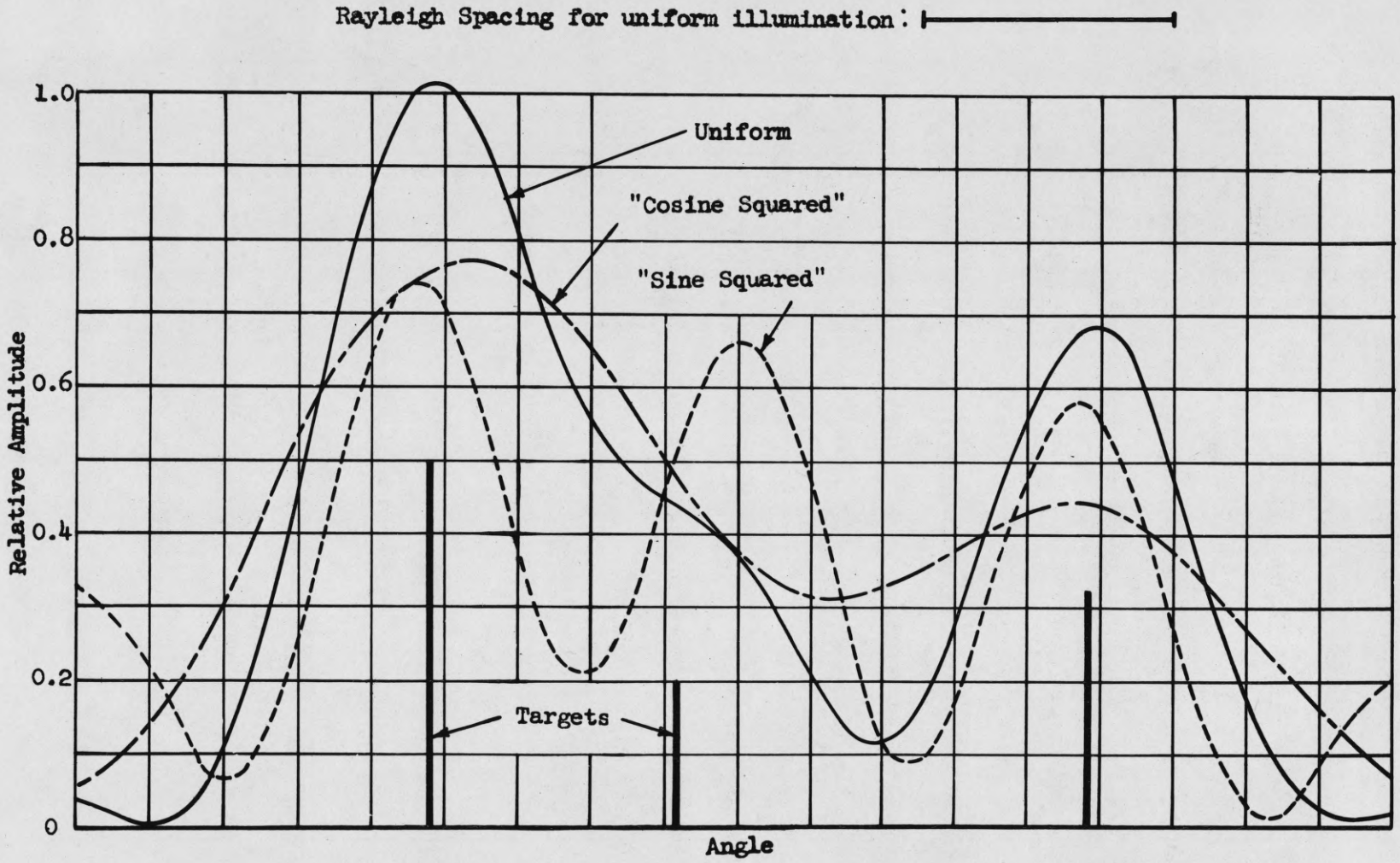

Typical images obtained from three point targets for three different antenna aperture illuminations.

Figure 1

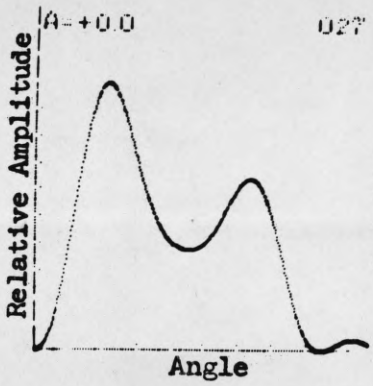

(a)

Image of three point targets formed by antenna with uniform aperture illumination.

FIRST MAJOR CYCLE

SECOND MAJOR CYCLE

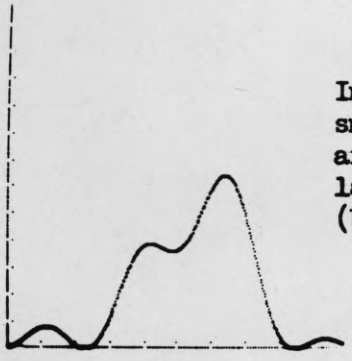

(b)

Image due to two smallest targets after removal of largest target (by 3rd estimate),

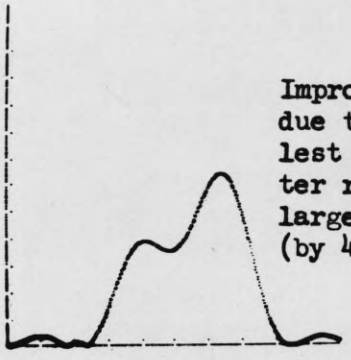

(e)

Improved image due to two smallest targets after removal of largest target (by 4th estimate).

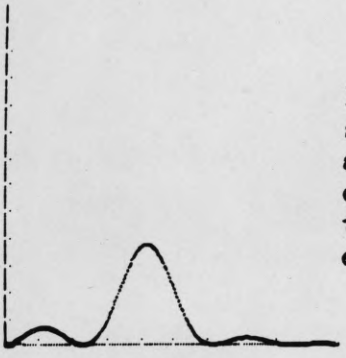

(c)

Image due to smallest target after removal of two largest targets (by 3rd estimate).

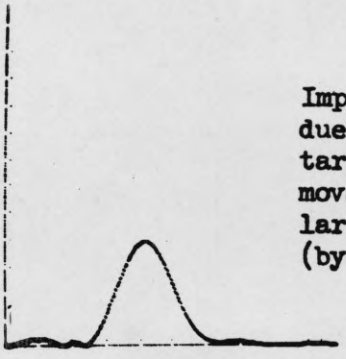

(f)

Improved image due to smallest target after removal of two largest targets (by 4th estimate).

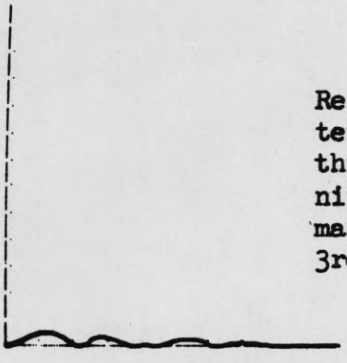

(d)

Residual left after removal of three targets. Finite residual remains due to inexact 3rd estimates.

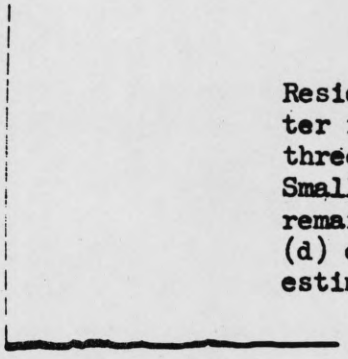

(g)

Residual left after removal of three targets. Smaller residual remains than in (d) due to improved estimates.

Photographs of cathode-ray tube output from ILLIAC showing the essence of the "deconvolution" process used by the Mechanical Observer in assessing image quality. The image in (a) is typical of the type containing "hidden" targets which may be revealed by the technique employed.

Figure 2

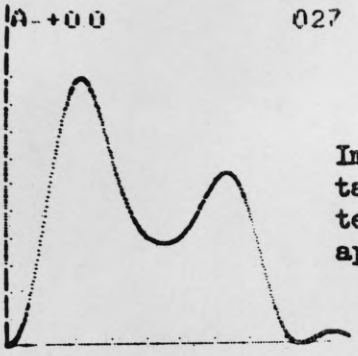

(a)

Image of three point targets formed by antenna with uniform aperture illumination.

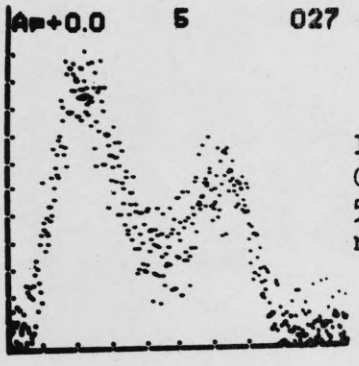

(b)

Image of (a) with Gaussian noise of 5:1 signal-to-noise ratio added.

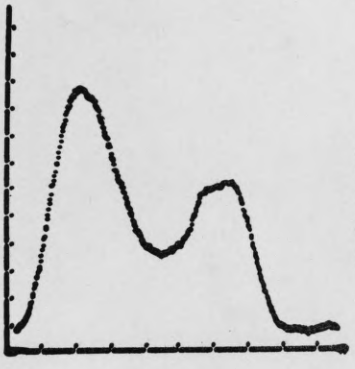

(c)

Image of (b) after smoothing by running mean of 25 ordinates.

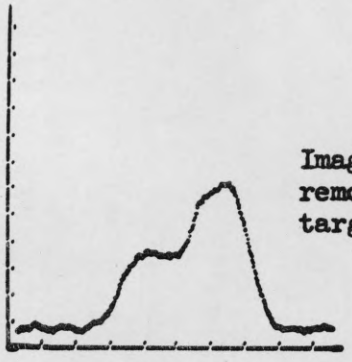

(d)

Image of (c) after removal of largest target.

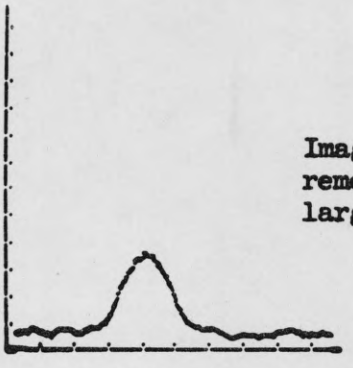

(e)

Image of (c) after removal of two largest targets.

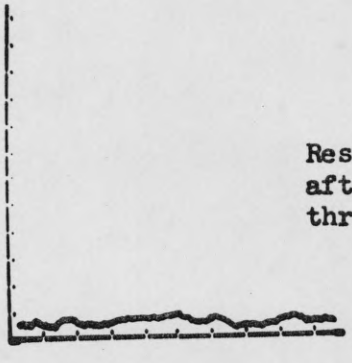

(f)

Residual of (c) after removal of three targets.

Photographs of cathode-ray tube output from ILLIAC showing the "deconvolution" process in the presence of noise introduced by adding random numbers to the image ordinates. Only the results of the first major cycle are shown (see Fig. 2 for more detail).

Figure 3

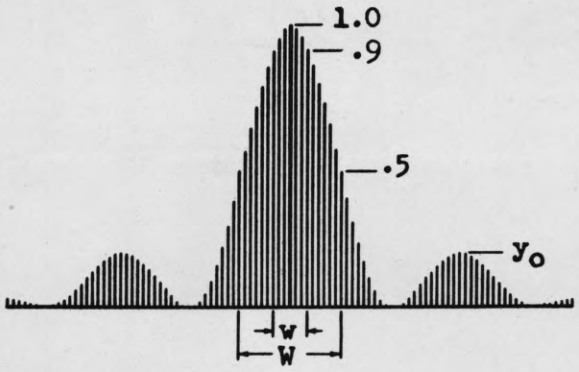

(a) Reference antenna pattern.

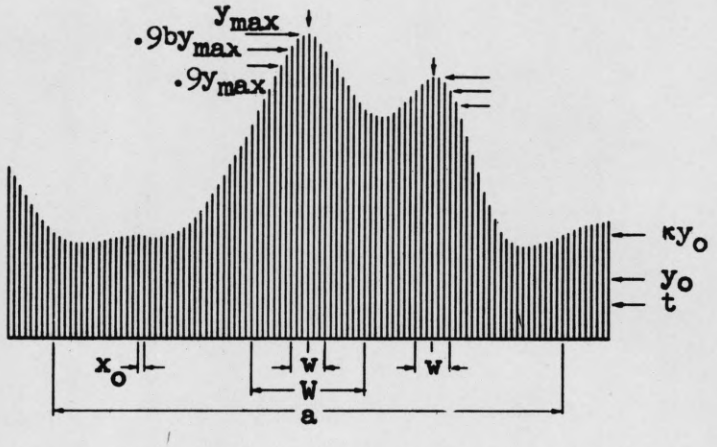

(b) Typical section of image showing two probable targets.

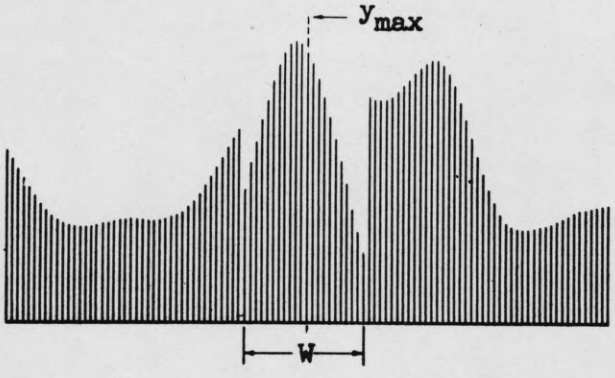

(c) Same as (b) after subtraction of interfering contributions to image in vicinity of largest target due to nearby targets.

Representation of typical data manufactured by ILLIAC and used by Mechanical Observer. Quantization in the x-coordinate is shown; parameters indicated are referred to in Appendix.

Figure 4

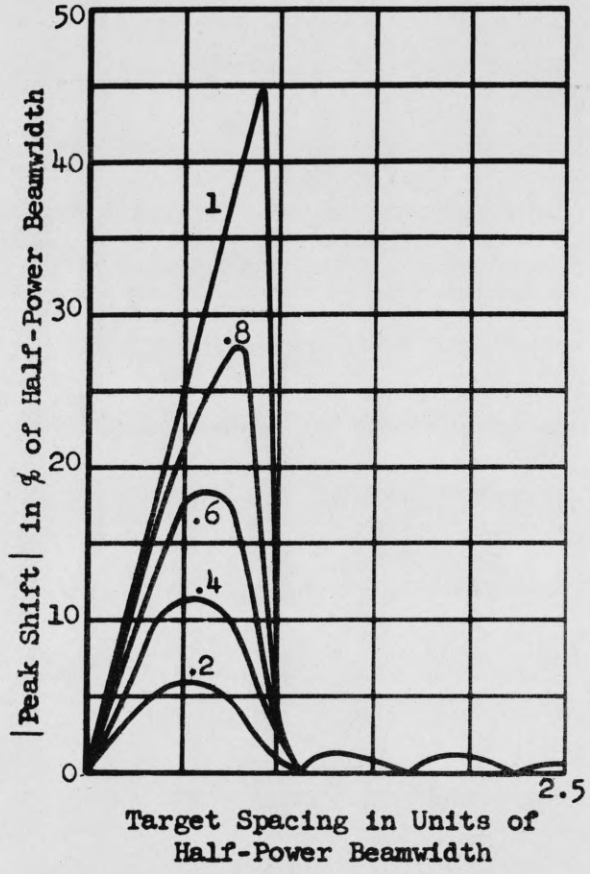

(a) Shift in apparent position of point target due to proximity of a second point target, for several different amplitudes of second target. Antenna power pattern is that for uniform illumination.

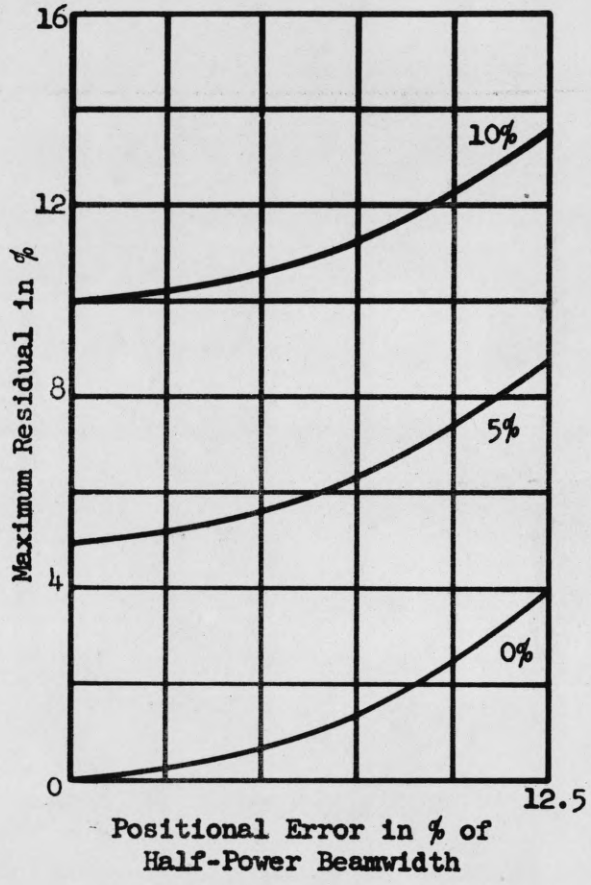

(b) Magnitude of maximum residual after subtraction of antenna power radiation pattern from itself, as a function of positional error, for three amplitude errors. Antenna pattern for uniform illumination.

Subtraction errors in Mechanical Observer

Figure 5

Target amplitude ratio 1:1 — — — —
Target amplitude ratio 2:1 ————————
Target amplitude ratio 5:1 — — — — — —

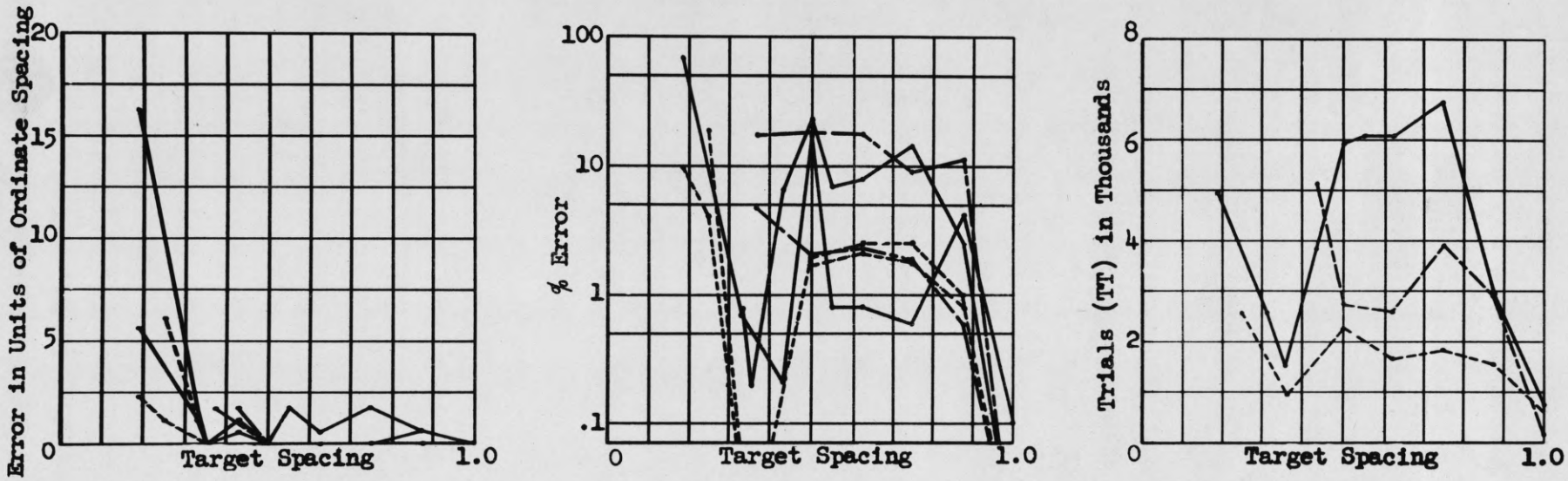

(a) Position error

(b) Amplitude error

(c) Number of trials

Aperture illumination factor
A = -1.0

Experimental results obtained using the Mechanical Observer to "deconvolve" image of two point targets. Target spacing is expressed in units of Rayleigh Spacing for "cosine-squared" illumination (A = 1.0). For each target amplitude ratio there are shown two curves on each graph; in general, the lower curve is for the first target found.

Figure 6

Target amplitude ratio 1:1 ——— - ——— -
Target amplitude ratio 2:1 ———————
Target amplitude ratio 5:1 - - - - - - -

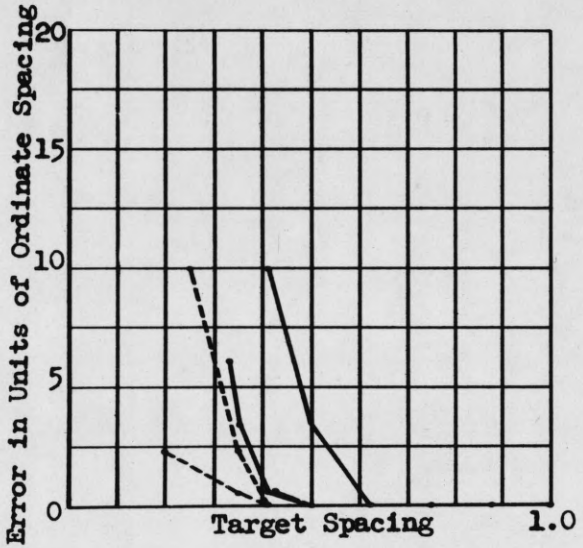

(a) Position error

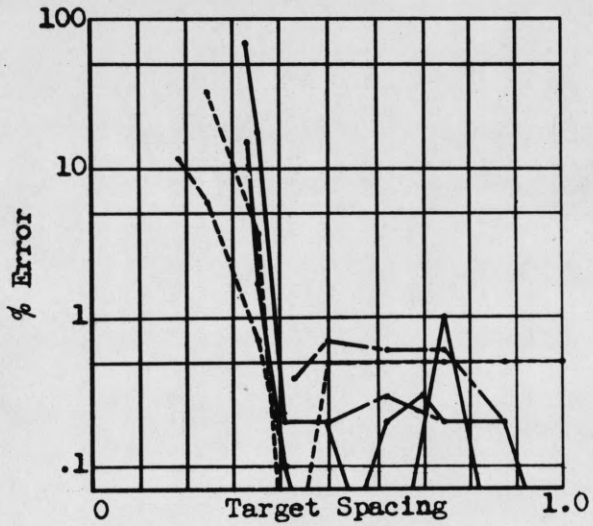

(b) Amplitude error

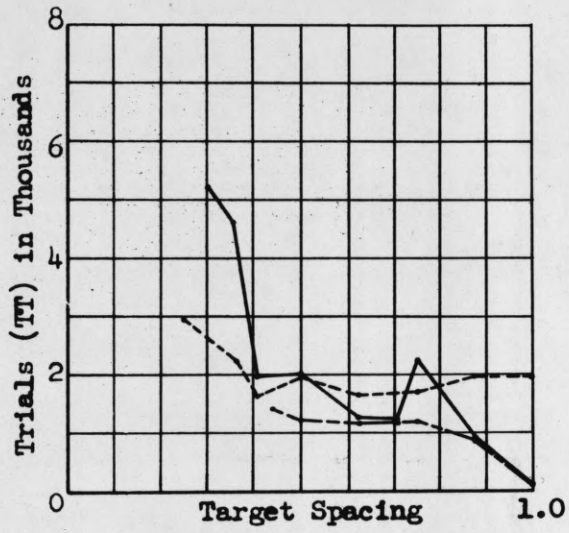

(c) Number of trials

Aperture illumination factor
A = -0.5

Experimental results obtained using the Mechanical Observer to "deconvolve" image of two point targets. See caption of Fig. 6.

Figure 7

Target amplitude ratio 1:1 ——— - ——— -
Target amplitude ratio 2:1 ———————
Target amplitude ratio 5:1 - - - - - - -

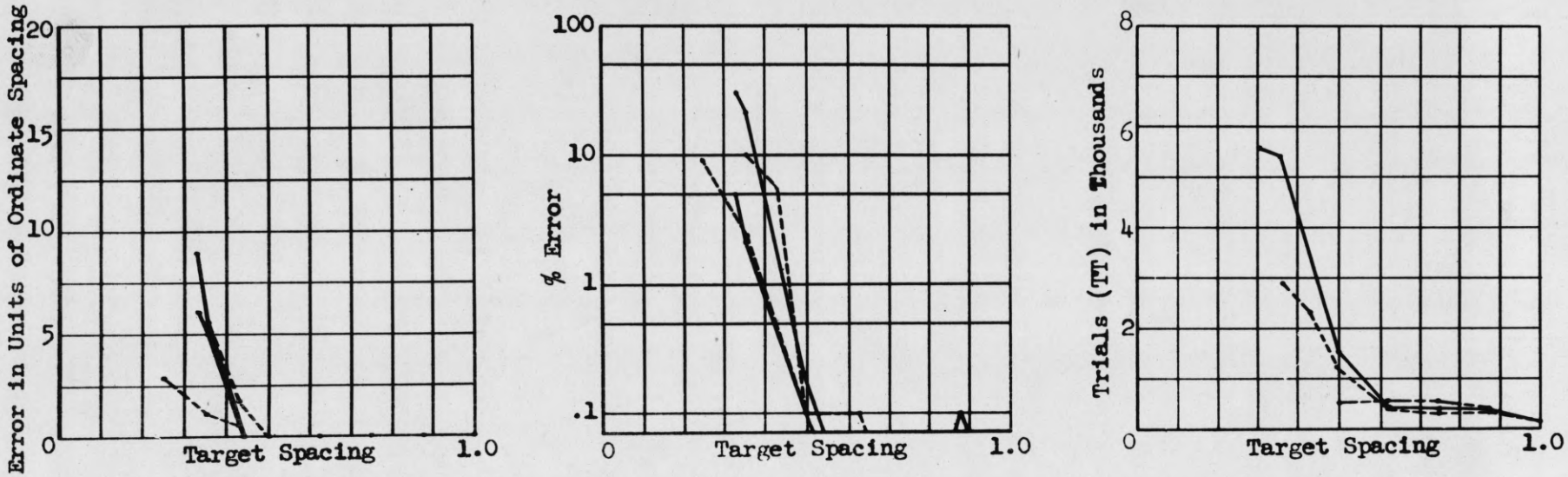

Aperture illumination factor
A = 0.1

Experimental results obtained using the Mechanical Observer to "deconvolve" image of two point targets. See caption of Fig. 6.

Figure 8

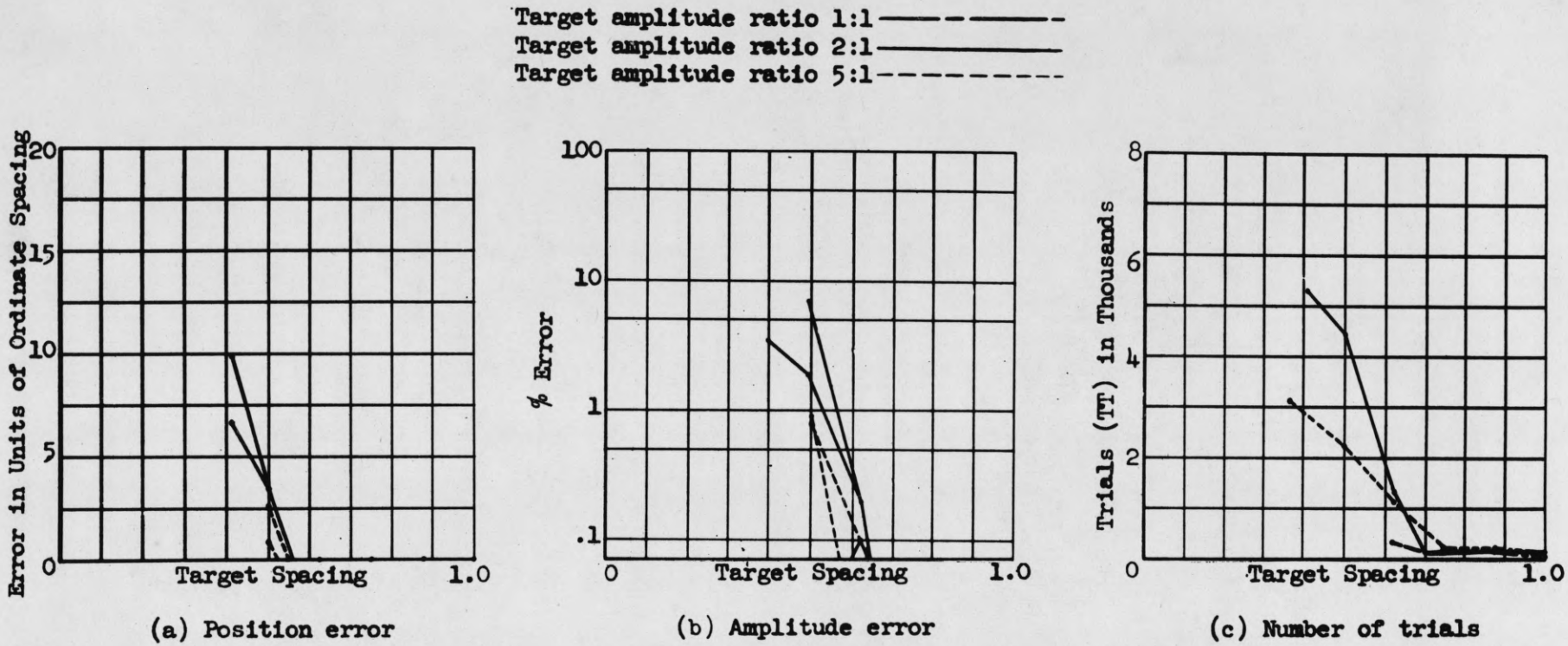

Aperture illumination factor
A = 0.5

Experimental results obtained using the Mechanical Observer to "deconvolve" image of two point targets. See caption of Fig. 6.

Figure 9

Target amplitude ratio 1:1 ——— - ——— -
Target amplitude ratio 2:1 ———————
Target amplitude ratio 5:1 - - - - - - - -

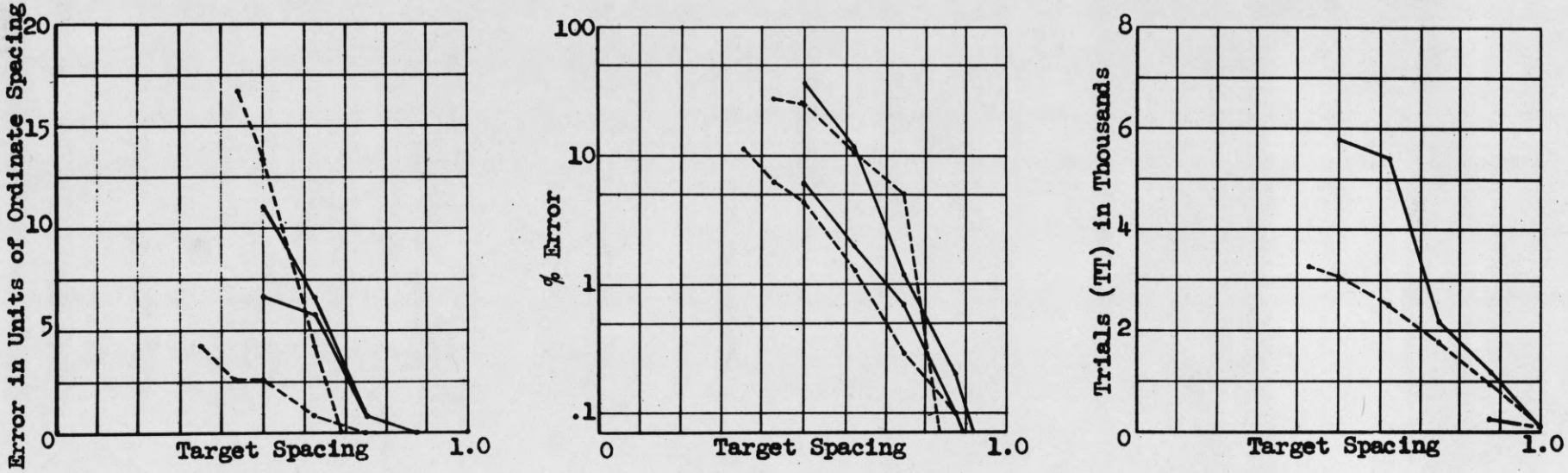

(a) Position error

(b) Amplitude error

(c) Number of trials

Aperture illumination factor
A = 1.0

Experimental results obtained using the Mechanical Observer to "deconvolve" image of two point targets. See caption of Fig. 6.

Figure 10

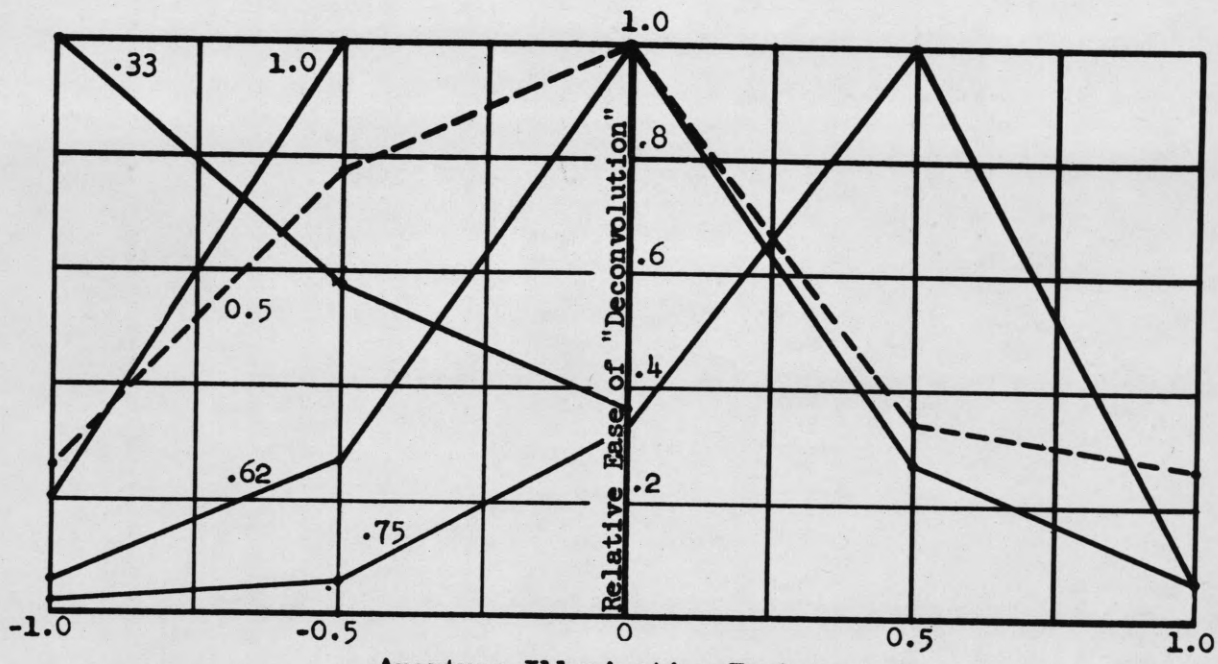

(a) Target amplitude ratio 2:1

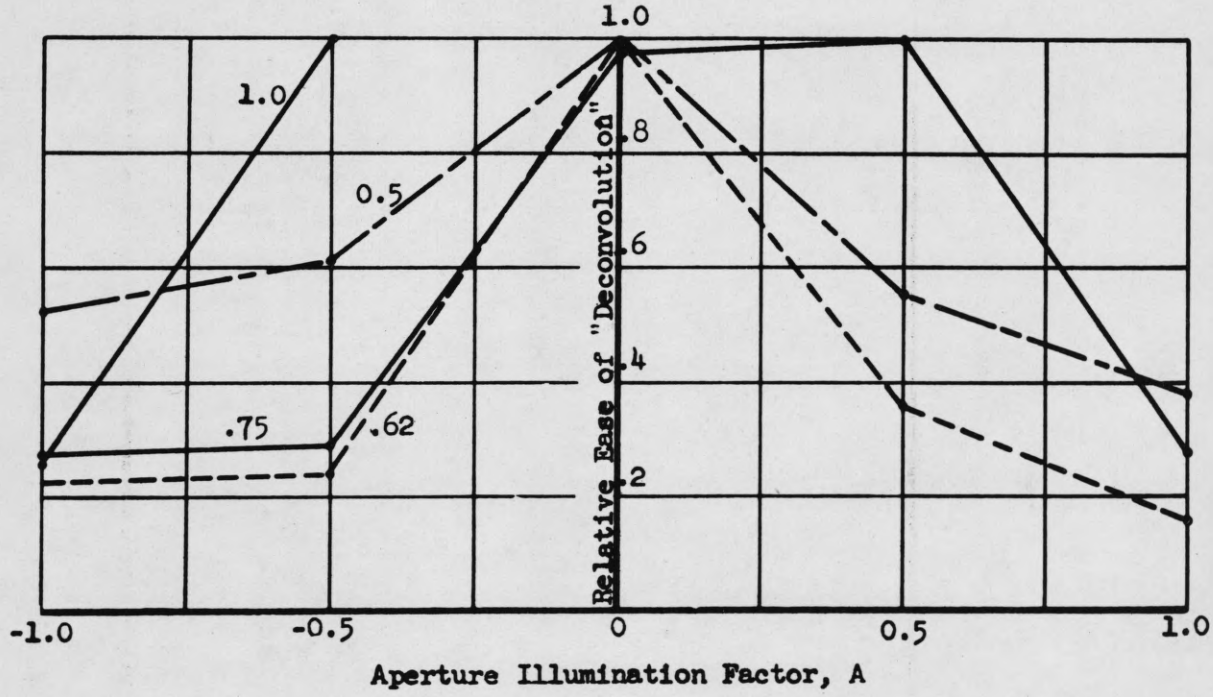

(b) Target amplitude ratio 5:1

Relative ease with which Mechanical Observer "deconvolves" image due to two point targets, as measured by number of trials. The various curves correspond to the indicated target spacings in units of Rayleigh Spacing for a "cosine-squared" illumination (A = 1.0).

Figure 11

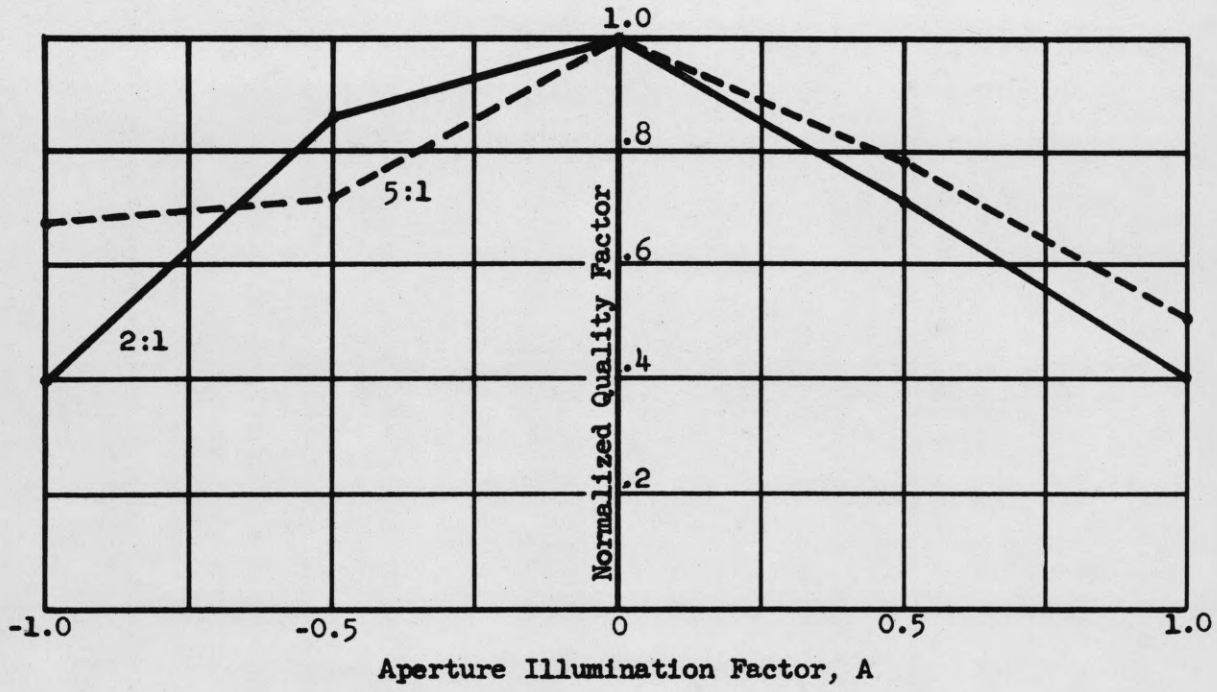

(a) Overall image quality

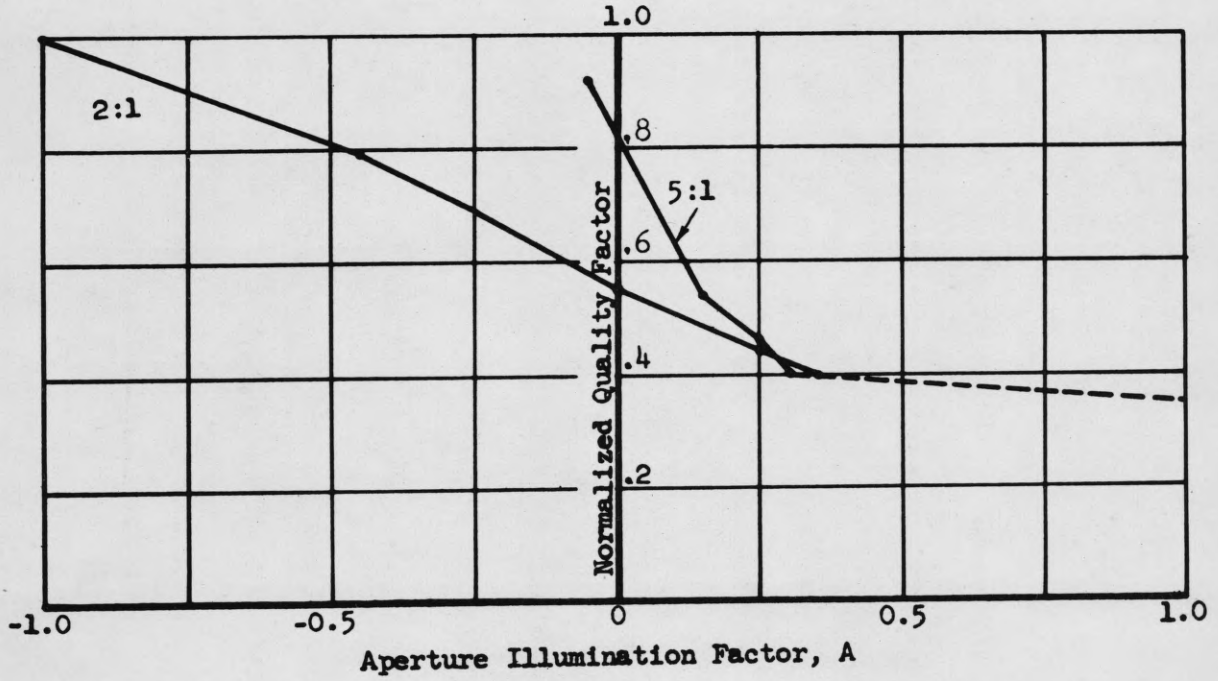

(b) Resolution

Relative overall image quality and resolution quality for aperture illumination $(1 + A \cos 2\pi x/L)$ as determined by Mechanical Observer, for two ratios of target amplitudes. In (a), each curve has been normalized so that 1.0 represents the best illumination of the class; in (b), the curve for 5:1 ratio has been normalized by the same factor used for normalizing the 2:1 ratio curve.

Figure 12

SER. 2 4 9

A = −.5

NOISE = .Ø PERCENT NO 1

1ST EST		2ND EST		CONST	TT
1.Ø95	91	.941	9Ø	.Ø211	67Ø
.5Ø7	217	.5Ø7	217	−.ØØØ6	72

3RD EST		4TH EST		CONST	TT
.962	9Ø	.997	9Ø	.ØØ7Ø	349
.5Ø7	217	.5ØØ	217	−.ØØ33	175

Print of punched tape output from ILLIAC mechanized observer used to "deconvolve" two-target image. The 4TH EST is the final result.

Figure 13

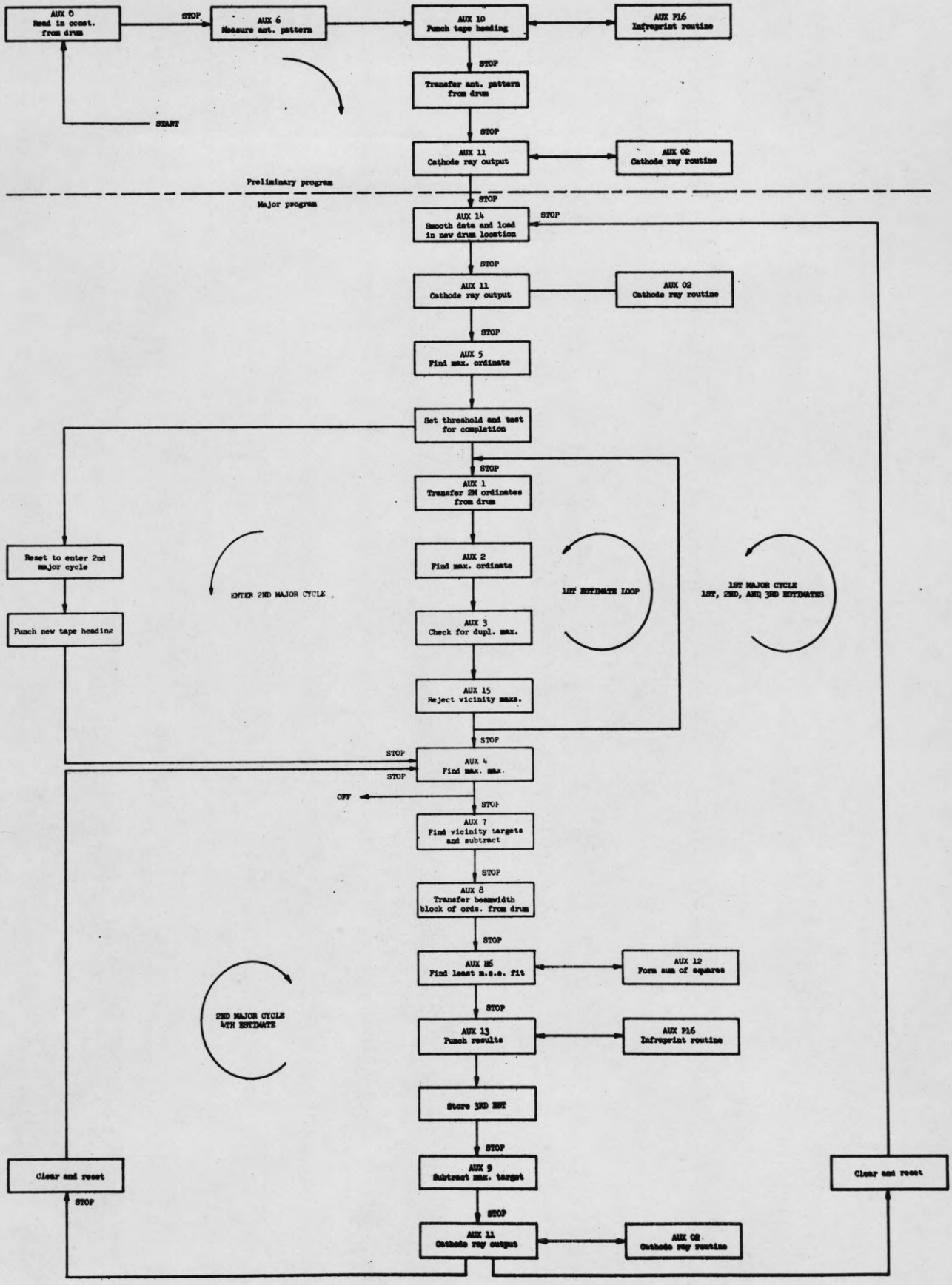

Simplified block diagram of ILLIAC program for Mechanical Observer

Figure 14

AUTHORIZED DISTRIBUTION LIST

Number of Copies	Agency
3	Director Ballistics Research Laboratory Aberdeen Proving Ground, Maryland Attn: Dr. L. A. Delsasso
1	Commander United States Air Force Security Service San Antonio, Texas Attn: CLR
1	Headquarters, Air Force Office of Scientific Research Air Research and Development Command United States Air Force Washington 25, D. C. Attn: SROP
1	Commander Headquarters, Air Research and Development Command P. O. Box 1395 Baltimore 3, Maryland Attn: RDDDR-5
1 Progress Reports Only	Air Force Ballistic Missile Division Headquarters, Air Research and Development Command, USAF P. O. Box 262 Inglewood, California Attn: WDSOT-8-18777
1	Commander Air Force Cambridge Research Center Laurence G. Hanscom Field Bedford, Massachusetts Attn: CRR
1 1	Director of Research and Development Headquarters, United States Air Force Washington 25, D. C. Attn: AFDRD-AC/2 AFDRD-CC/2
2 Progress Reports Only	U. S. Navy Inspector of Ordnance Applied Physics Laboratory The Johns Hopkins University 8621 Georgia Avenue Silver Springs, Maryland
10	Armed Services Technical Information Agency Arlington Hall Station Arlington 12, Virginia

Number of Copies	Agency
1	President, U. S. Army Airborne and Electronics Board Continental Army Command Fort Bragg, North Carolina
1	President, U. S. Army Defense Board Continental Army Command Fort Bliss, Texas
1	Chief of Research and Development Office of the Chief of Staff Department of the Army Washington 25, D. C.
	Office of the Chief of Ordnance Department of Ordnance Washington 25, D. C.
1	Attn: ORDTR
1	ORDTB
	Department of the Army Office of the Chief Signal Officer Washington 25, D. C.
1	Attn: SIGRD
1	SIGRD-9-b
1	Commanding Officer
No Progress Reports	Office of Ordnance Research 2127 Myrtle Drive Duke Station Durham, North Carolina
1	Commanding General U. S. Continental Army Command Fort Monroe, Virginia Attn: Deputy Chief of Staff Material Development
1	Mr. A. A. Lundstrom Bell Telephone Laboratories Whippany, New Jersey
1	Chicago Midway Labs 6040 South Greenwood Avenue Chicago 37, Illinois Attn: Librarian
1	Joseph P. Desmond, Librarian Cornell Aeronautical Laboratory Buffalo, New York
1	Commanding Officer and Director David Taylor Model Basin Washington 7, D. C. Attn: Code 800

Number of Copies	Agency
1	Technical Library Code 142 David Taylor Model Basin Washington 7, D. C.
1	Commander Air Force Armament Center Eglin Air Force Base, Florida Attn: Deputy for Operations
1	9560 S. C. Electronics Research Unit P. O. Box 205 Mountain View, California
20	Transportation Officer Fort Monmouth Little Silver, New Jersey Marked for: USASROL Accountable Property Officer Building 2700 Camp Wood Area Inspect at Destination File No. 0060-PH-54-91(5308)
1	Commanding Officer Frankford Arsenal Philadelphia 37, Pennsylvania
1	General Electric Company Defense Electronics Center Cornell University Ithaca, New York Attn: Mr. Leonard Bigelow
1	Light Military Electronic Equipment Department General Electric Company French Road Utica, New York For: Contract AF 33(600)-16934
1	Goodyear Aircraft Corporation Akron 15, Ohio For: Project MX 778 Contract W33-038 ac-14153
1	Hughes Research and Development Library Hughes Aircraft Company Culver City, California Attn: Miss Mary Jo Case
1	Director Jet Propulsion Laboratory California Institute of Technology Pasadena, California

Number of Copies	Agency
1	Operations Research Office The Johns Hopkins University 6935 Arlington Road Bethesda, Maryland Attn: Document Control Office
1	Litton Industries 336 North Foothill Road Beverly Hills, California Via: Inspector of Naval Materiel Los Angeles, California
1	Librarian Instrumentation Laboratory Massachusetts Institute of Technology Cambridge 39, Massachusetts
1	Massachusetts Institute of Technology Lincoln Laboratory P. O. Box 73 Lexington 73, Massachusetts
1	Mr. Robert R. Everett Division Head Lincoln Laboratory Massachusetts Institute of Technology Lexington 73, Massachusetts
1	W. L. Maxson Corporation 460 West 34th Street New York 1, New York
1	Director Air University Library Maxwell Air Force Base, Alabama Attn: CR-4803a
1	Technical Documents Service Willow Run Laboratories University of Michigan Willow Run Airport Ypsilanti, Michigan
1	Commanding Officer Naval Air Development Center Johnsville, Pennsylvania Attn: Code AAEL
	Commanding Officer and Director U. S. Naval Electronics Laboratory San Diego 52, California
1	Attn: Library
1	Code 2800, C. S. Manning

Number of Copies	Agency
	Chief of Naval Operations Navy Department Washington 25, D. C.
1	Attn: OP-51
1	OP-91
1	OP-551
1	OP-345
1	Commander Naval Ordnance Laboratory White Oaks Silver Springs 19, Maryland Attn: Technical Library
1	Naval Ordnance Proving Ground Computation Center Dahlgren, Virginia Attn: R. A. Niemann
1	Commanding Officer Office of Naval Research Chicago Branch John Crerar Library Building 10th Floor, 86 East Randolph Street Chicago 1, Illinois
	Department of the Navy Office of Naval Research Washington 25, D. C.
1	Attn: Code 900
1	Code 430
2	Code 437
1	Director Office of Naval Research Branch Office 1000 Geary Street San Francisco, California
	Director Naval Research Laboratory Washington 25, D. C.
3	Attn: Code 5140
	Chief, Bureau of Aeronautics Department of the Navy Washington 25, D. C.
1	Attn: EL-402
1	TD-4
1	Bureau of Ordnance Department of the Navy Washington 25, D. C. Attn: Re4C

Number of Copies	Agency
	Chief, Bureau of Ships Department of the Navy Washington 25, D. C.
2	Attn: Code 280
1	Code 565C
1	Code 810
1	Code 810B
1	Code 812
1	Code 820
1	Code 825
1	Code 830
1	Code 835
1	Head, Combat Direction Systems Branch (OP-345) Department of the Navy Room 4C-518 Pentagon Washington 25, D. C.
5 Progress Reports Only	National Aeronautics and Space Administration 1520 H. Street Northwest Washington 25, D. C.
1	Director National Bureau of Standards Washington 25, D. C. Attn: Dr. S. N. Alexander
1	Radio Corporation of America RCA Laboratories Division David Sarnoff Research Center Princeton, New Jersey Attn: Mr. A. W. Vance
1	The Rand Corporation 1700 Main Street Santa Monica, California Attn: Library
2	Commanding General Redstone Arsenal Huntsville, Alabama Attn: Technical Library
1	Remington Rand Univac Division of Sperry Rand Corporation Via: Insmat, BuShips Insp. Officer 1902 West Minnehaha Avenue St. Paul 4, Minnesota
1	Commanding Officer Rome Air Development Center Griffiss Air Force Base, New York

Number of Copies	Agency
1	Stanford University Electronics Research Laboratory Stanford, California
1	System Development Corporation 2500 Colorado Avenue Santa Monica, California
1	Sylvania Electric Products, Inc. 100 First Avenue Waltham 54, Massachusetts Attn: Contract DA-30-069-ORD-1166
	Commander Wright Air Development Center Wright-Patterson Air Force Base, Ohio
2	Attn: WCOSI-3
1	WCLOT-2
1	WCLCR-4
1	WCLG
1	WCLJY
1	WCLGN-5
1	WCLR
1	WCLRW-1
1	WCLJ
1	WCLRW-2